Natural Modes in Three-dimensional Rectangular Moonpools with Recess in Finite-depth Waters

Xinshu Zhang*, Zhanghanyi Li, Jian Han

State Key Laboratory of Ocean Engineering, Shanghai Jiao Tong University, Shanghai 200240, China

1 Introduction

'Moonpools' are vertical openings, through the deck and hull of ships or offshore oil and gas exploration platforms, designed for marine and offshore operations such as pipe laying, riser hang-off or diver recovery. As being exposed to incident waves or harmonic ship motions, the fluid inside moonpool may perform significant resonant motions. Since the large fluid motions inside moonpools can cause negative impacts, it is important to predict the resonance frequencies and modal shapes of free-surface elevation at the design stage. The natural modes in a moonpool consist of sloshing modes and piston mode, where the entrapped water heaves up and down more or less like a solid.

Molin (2001) developed an ingenious method to solve the moonpool resonance problem, based on the assumption that the water depth is infinite and the beam/length are very large. A series of formulations have been derived to predict the natural frequencies. More recently, new models (Molin *et al.*, 2018; Zhang *et al.*, 2019) have been developed to study three-dimensional and two-dimensional moonpool resonances in finite-depth waters and demonstrate that the solutions can be improved significantly comparing to the previous models. In the present study, we develop a model to predict the natural frequencies and modal shapes for three-dimensional rectangular moonpools with recess in finite-depth waters. We examine the effects of recess on resonant wave motion, including natural frequencies and modes.

2 Mathematical Formulation

We developed a new model to study the natural modes of a three-dimensional moonpool with recess. The sketch of the problem is illustrated in Fig. 1. It is assumed that the flow inside the moonpool to be three-dimensional. Based on domain-decomposition scheme, three subdomains are defined as illustrated in Fig. 1. The origin of the coordinate system is placed at the left corner of the recess. The horizontal dimension of the moonpool is L_2 by B_2. The moonpool height is d_1 and the recess height is d_2. The horizontal dimension of the recess is b_1 by b_2. The key assumption here is that velocity potential is nil at the outer boundaries (T_1, T_2, T_3 and T_4 as denoted in the sketch). c is the clearance between the bottom of the supporting structure and the seabed.

The velocity potential in the subdomain 1 (inside moonpool) is taken as

$$\varphi_1(x,y,z) = A_{00} + B_{00}\frac{z-d_2}{d_1} + \sum_{m=0}^{\infty}\sum_{\substack{n=0\\(m,n)\neq(0,0)}}^{\infty}[A_{mn}\cosh\nu_{mn}(z-d_2)$$

$$+B_{mn}\sinh\nu_{mn}(z-d_2)]\cos\lambda_m(x+b_1)\cos\mu_n(y+b_2) \qquad (1)$$

with $\lambda_m = m\pi/L_2$, $\mu_n = n\pi/B_2$, $\nu_{mn}^2 = \lambda_m^2 + \mu_n^2$; m and n are integers. $b_1 = (L_2 - L_3)/2$ and $b_2 = (B_2 - B_3)/2$.
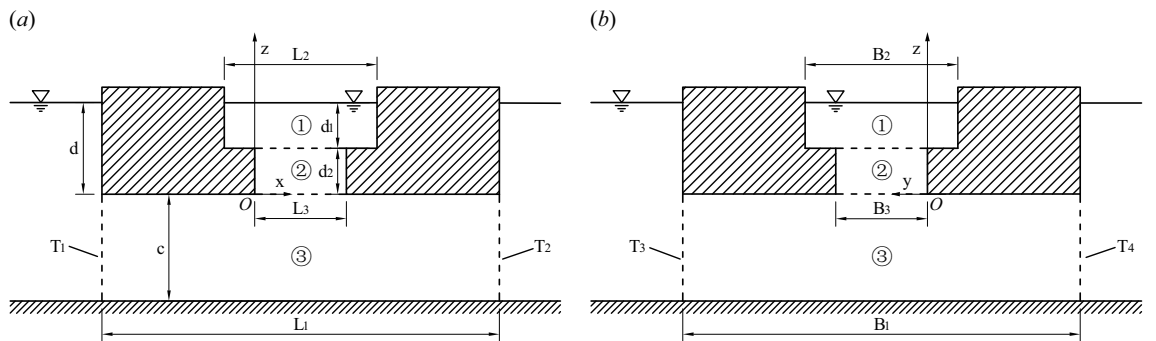
Figure 1: Sketch of the problem and coordinate system. (*a*) and (*b*) are the two sideview.

---

*Corresponding author, Innovative Marine Hydrodynamics Lab, SJTU (xinshuz@sjtu.edu.cn)

In the subdomain 2 which is inside the recess as shown in Fig. 1, the velocity potential is written as

$$\varphi_2(x, y, z) = C_{00} + D_{00}\frac{z}{d_2} + \sum_{p=0}^{\infty} \sum_{\substack{q=0 \\ (p,q)\neq(0,0)}}^{\infty} [C_{pq}\cosh\gamma_{pq}z + D_{pq}\sinh\gamma_{pq}z]\cos\alpha_p x \cos\beta_q y \tag{2}$$

with $\alpha_p = p\pi/L_3$, $\beta_q = q\pi/B_3$, p and q are integers, and $\gamma_{pq}^2 = \alpha_p^2 + \beta_q^2$.

In the subdomain 3 which is underneath the moonpool, the velocity potential is taken as

$$\varphi_3(x, y, z) = \sum_{i=1}^{\infty}\sum_{j=1}^{\infty} E_{ij}\frac{\cosh\sigma_{ij}(z+c)}{\cosh\sigma_{ij}c}\sin\kappa_i(x+a_1)\sin\tau_j(y+a_2) \tag{3}$$

with $\kappa_i = i\pi/L_1$, $\tau_j = j\pi/B_1$, $\sigma_{ij}^2 = \kappa_i^2 + \tau_j^2$, i and j are the integers. $a_1 = (L_1 - L_3)/2$, $a_2 = (B_1 - B_3)/2$.

With these expansions the Laplace equation and the boundary conditions at the vertical boundaries are fulfilled. It remains to match the velocity potential and velocity at the common boundaries. We apply Garrett's method (Garrett, 1971) in the following.

Matching of the potential and vertical velocity on $z = d_2$

It must be ensured that

$$A_{00} + \sum_{m=0}^{\infty}\sum_{\substack{n=0 \\ (m,n)\neq(0,0)}}^{\infty} A_{mn}\cos\lambda_m(x+b_1)\cos\mu_n(y+b_2) = C_{00} + D_{00}$$

$$+ \sum_{p=0}^{\infty}\sum_{\substack{q=0 \\ (p,q)\neq(0,0)}}^{\infty} (C_{pq}\cosh\gamma_{pq}d_2 + D_{pq}\sinh\gamma_{pq}d_2)\cos\alpha_p x \cos\beta_q y \tag{4}$$

Multiply both sides with $\cos\alpha_p x \cos\beta_q y$ and integrate with x and y over the moonpool, we get

$$C_{00} + D_{00} = A_{00} + \sum_{m=0}^{\infty}\sum_{\substack{n=0 \\ (m,n)\neq(0,0)}}^{\infty} \frac{A_{mn}}{L_3 B_3}\int_0^{L_3}\cos\lambda_m(x+b_1)\,\mathrm{d}x\int_0^{B_3}\cos\mu_n(y+b_2)\,\mathrm{d}y \tag{5}$$

and

$$C_{pq} + D_{pq}\tanh\gamma_{pq}d_2 = \sum_{m=0}^{\infty}\sum_{\substack{n=0 \\ (m,n)\neq(0,0)}}^{\infty} \frac{\xi_{pq}A_{mn}}{L_3 B_3\cosh\gamma_{pq}d_2}\int_0^{L_3}\cos\lambda_m(x+b_1)\cos\alpha_p x\,\mathrm{d}x\int_0^{B_3}\cos\mu_n(y+b_2)\cos\beta_q y\,\mathrm{d}y \tag{6}$$

which can be written in matrix form as

$$\vec{C} + \boldsymbol{D_D}\vec{D} = \boldsymbol{M_A}\vec{A} \tag{7}$$

where $\boldsymbol{D_D}$ the diagonal matrix and $\boldsymbol{M_A}$ is a full matrix. If p or $q = 0$, then $\xi_{pq} = 2$, otherwise $\xi_{pq} = 4$.

In addition, the continuity condition of vertical velocity gives

$$\frac{\partial\varphi_1(x,y,z)}{\partial z} = \frac{\partial\varphi_2(x,y,z)}{\partial z}, 0 \leq x \leq L_3, 0 \leq y \leq B_3, \tag{8}$$

$$= 0 \text{ elsewhere.} \tag{9}$$

That is

$$\frac{B_{00}}{d_1} + \sum_{m=0}^{\infty}\sum_{\substack{n=0 \\ (m,n)\neq(0,0)}}^{\infty} B_{mn}\nu_{mn}\cos\lambda_m(x+b_1)\cos\mu_n(y+b_2) =$$

$$\frac{D_{00}}{d_2} + \sum_{p=0}^{\infty}\sum_{\substack{q=0 \\ (p,q)\neq(0,0)}}^{\infty} \gamma_{pq}(D_{pq}\cosh\gamma_{pq}d_2 + C_{pq}\sinh\gamma_{pq}d_2)\cos\alpha_p x \cos\beta_q y. \tag{10}$$

By a similar procedure, we can obtain the following vectorial form

$$\vec{B} = \boldsymbol{M_{BC}}\vec{C} + \boldsymbol{M_{BD}}\vec{D} \tag{11}$$

Matching of the potential and vertical velocity on $z = 0$

It must be ensured that

$$C_{00} + \sum_{\substack{p=0 \\ (p,q)\neq(0,0)}}^{\infty} \sum_{q=0}^{\infty} C_{pq}\cos\alpha_p x\cos\beta_q y \quad = \quad \sum_{i=1}^{\infty}\sum_{j=1}^{\infty} E_{ij}\sin\kappa_i(x+a_1)\sin\tau_j(y+a_2) \tag{12}$$

Multiply each side with $\cos\alpha_p x\cos\beta_q y$ and integrate over the domain of validity, we obtain

$$\overrightarrow{C} = \boldsymbol{M_{CE}}\overrightarrow{E} \tag{13}$$

In order to match the vertical velocity, it must be ensured that

$$\sum_{i=1}^{\infty}\sum_{j=1}^{\infty} E_{ij}\sigma_{ij}\tanh\sigma_{ij}c\sin\kappa_i(x+a_1)\sin\tau_j(y+a_2) = \frac{D_{00}}{d_2} + \sum_{\substack{p=0 \\ (p,q)\neq(0,0)}}^{\infty}\sum_{q=0}^{\infty} D_{pq}\gamma_{pq}\cos\alpha_p x\beta_q y \tag{14}$$

By a similar procedure, we get

$$\overrightarrow{E} = \boldsymbol{M_{ED}}\overrightarrow{D} \tag{15}$$

By combing (13) and (15), it yields

$$\overrightarrow{C} = \boldsymbol{M_{CE}}\cdot\boldsymbol{M_{ED}}\overrightarrow{D} = \boldsymbol{M_{CD}}\overrightarrow{D} \tag{16}$$

By substituting (1) into the free-surface boundary condition, it gives

$$\frac{B_{00}}{d_1} + \sum_{m=0}^{\infty}\sum_{\substack{n=0 \\ (m,n)\neq(0,0)}}^{\infty} \nu_{mn}\left(A_{mn}\sinh\nu_{mn}d_1 + B_{mn}\cosh\nu_{mn}d_1\right) =$$

$$\frac{\omega^2}{g}\left(A_{00} + B_{00} + \sum_{m=0}^{\infty}\sum_{\substack{n=0 \\ (m,n)\neq(0,0)}}^{\infty}\left(A_{mn}\cosh\nu_{mn}d_1 + B_{mn}\sinh\nu_{mn}d_1\right)\right) \tag{17}$$

which can be written in vectorial form as

$$\boldsymbol{D_1}\overrightarrow{A} + \boldsymbol{D_2}\overrightarrow{B} = \omega^2(\overrightarrow{A} + \boldsymbol{D_4}\overrightarrow{B}) \tag{18}$$

with

$$\text{diag}\,\boldsymbol{D_1} \quad = \quad (0, g\nu_{mn}\tanh\nu_{mn}d_1) \tag{19}$$
$$\text{diag}\,\boldsymbol{D_2} \quad = \quad (g/d_1, g\nu_{mn}) \tag{20}$$
$$\text{diag}\,\boldsymbol{D_4} \quad = \quad (1, \tanh\nu_{mn}d_1) \tag{21}$$

By combing (7), (11), and (16), it yields

$$(\boldsymbol{D_1} + \boldsymbol{D_2}\cdot\boldsymbol{M_{BA}})\overrightarrow{A} = \omega^2(\boldsymbol{I} + \boldsymbol{D_4}\cdot\boldsymbol{M_{BA}})\overrightarrow{A} \tag{22}$$

with

$$\boldsymbol{M_{BA}} = (\boldsymbol{M_{BC}}\cdot\boldsymbol{M_{CD}} + \boldsymbol{M_{BD}})(\boldsymbol{M_{CD}} + \boldsymbol{D_D})^{-1}\boldsymbol{M_A} \tag{23}$$

where $\boldsymbol{I}$ is the identity matrix. The solution of this eigenvalue problem in (22) yields the natural frequencies and associated modal shapes of the free surface. In addition, following Molin (2017), we derived a frozen-mode approximation (FMA) model for finite-depth waters by assuming the fluid inside the recess moves up and down like a solid. The added-masses due to the fluid inside subdomain 1 and 3 are derived.

3   Results and Discussion

We study a floating foundation for wind turbine with a square moonpool, as described in Guignier *et al.* (2016), but with recess. Here, the objective to examine the effect of recess on the natural modes of a three-dimensional moonpool. We take the same dimensions of the floating foundation and moonpool as those in the initial design. The dimension of the recess in the x and y directions are taken to be the same, which means $L_3 = B_3$.

The present results by solving the eigenvalue problem and adopting the developed frozen-mode approximation model are compared with solutions using a diffraction-radiation code (WAMIT, 2016). Fig. 2(a) illustrates the variation of piston-mode frequency with respect to the horizontal dimension of the recess while the heigh of recess is fixed. Fig. 2(b) illustrates the effect of recess height on the piston-mode frequency and also shows

the comparison with the prediction by frozen-mode approximation. It's interesting to find that the results by frozen-mode approximation model agree quite well with the solutions by WAMIT. In order to illustrate the effect of recess on modal shapes of free surface, Fig. 3 present the modal shapes for moonpool w/o and with recess. As shown, in contrast to the case without recess, the free surface above the recess is relatively higher than that elsewhere. In particular, the free-surface elevations at the four corners reach the highest.

Finally, for the square moonpool with recess, we observe the modes $(2,0) + (0,2)$ and $(2,0) - (0,2)$, whose natural frequencies do not come to the same frequency in case of a square recess, similar to that reported in Molin *et al.* (2018). More detailed results will be reported during the workshop.
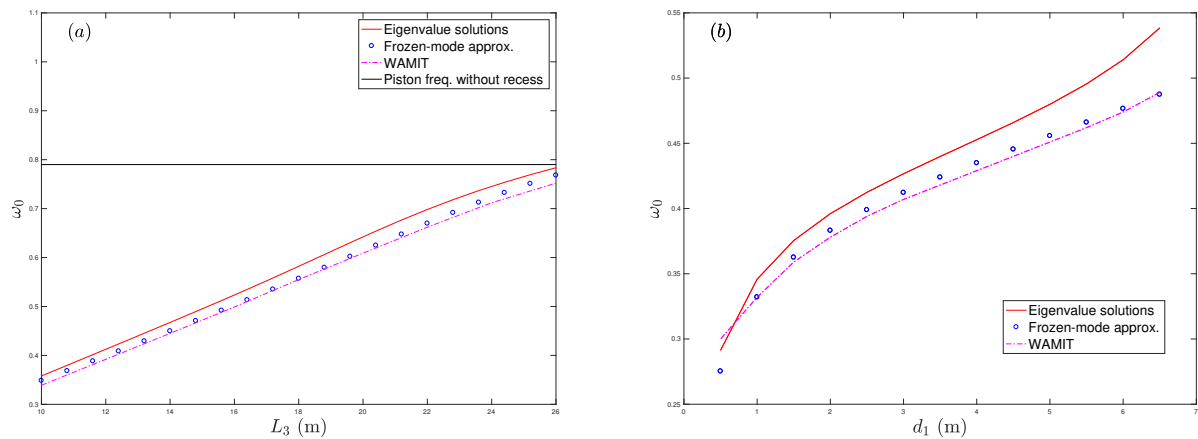
Figure 2: Square moonpool. (*a*) The variation of piston-mode frequency with respect to the L_3 (gap width inside recess). The height of moonpool $d_1 = 3.5$ m and height of recess is $d_2 = 3.5$ m; (*b*) The variation of piston-mode frequency with respect to the moonpool height d_1. The dimension of moonpool are 27 m by 27 m. Supporting structure is bounded by $L_1 = B_1 = 51$ m.
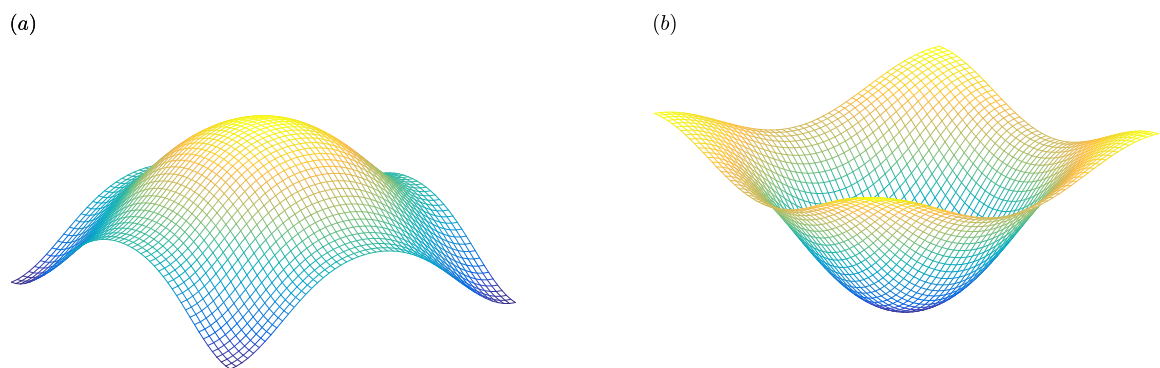
Figure 3: Modal shapes of free surface inside a square moonpool in piston-mode resonance. (*a*) without recess; (*b*) with recess. $L_3 = B_3 = 13$ m. $d_1 = d_2 = 3.5$ m.

References

GARRETT, C. J. R. 1971 Wave forces on a circular dock. *J. Fluid Mech.* **46**, 129–139.

GUIGNIER, L., COURBOIS, A., MARIANI, R. & CHOISNET, T. 2016 Multibody modelling of floating offshore wind turbine foundation for global loads analysis. In *Proceedings of the Twenty-sixth International Ocean and Polar Engineering Conference*.

MOLIN, B. 2001 On the piston and sloshing modes in moonpools. *J. Fluid Mech.* **430** (5), 27–50.

MOLIN, B. 2017 On natural modes in moonpools with recesses. *Appl. Ocean Res.* **67**, 1 – 8.

MOLIN, B., ZHANG, X., HUANG, H. & REMY, F. 2018 On natural modes in moonpools and gaps in finite depth. *J. Fluid Mech.* **840**, 530–554.

WAMIT, INC. 2016 *User Manual for WAMIT Version 7.2*. www.wamit.com/manual.htm.

ZHANG, X., HUANG, H. & SONG, X. 2019 On natural frequencies and modal shapes in two-dimensional asymmetric and symmetric moonpools in finite water depth. *Appl. Ocean Res.* **82**, 117 – 129.